厦门大学
XIAMEN UNIVERSITY

厦门大学环境与生态学院
COLLEGE OF THE ENVIRONMENT & ECOLOGY
XIAMEN UNIVERSITY

Gaseous mercury adsorption mechanism on carbon nanotubes with O-containing functional groups

JINJING LUO, SIQI ZHUO, MINGCHANG JIN

2024.7.26

1. Introdution

厦门大学环境与生态学院
COLLEGE OF THE ENVIRONMENT & ECOLOGY
XIAMEN UNIVERSITY

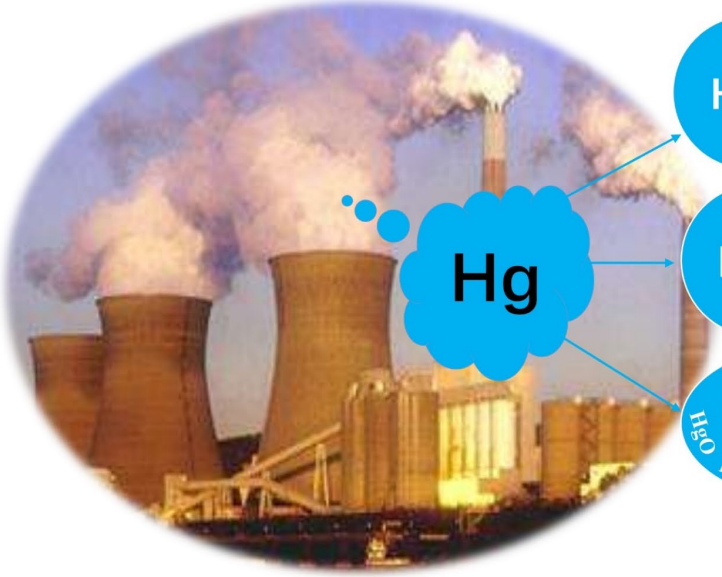

Hg^p ✔ Easy to deposit
Clothe bag deduster

Hg^0 Insoluble in water
Easy to volatilize ❓

Hg^{2+},Hg^+ HgO HgS $HgSO_4$ $HgCl_2$ ⋯ Can be dissolved in water
✔ *Wet desulfurization*

Surface modification

halide, sulfur, acid, alkaline, metal, metal oxides, microwave, plasma…

Modified Bio-char

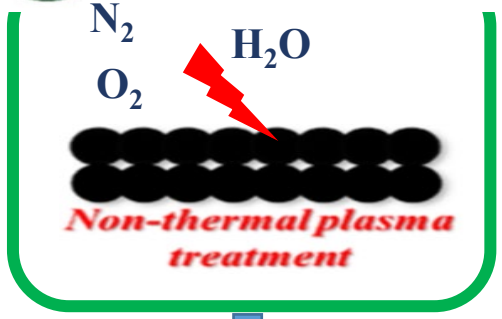

C-OCFGs

C-Cl

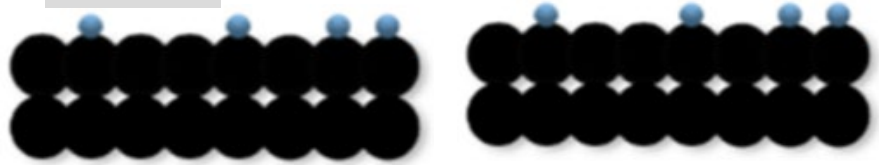

Modified bio-char

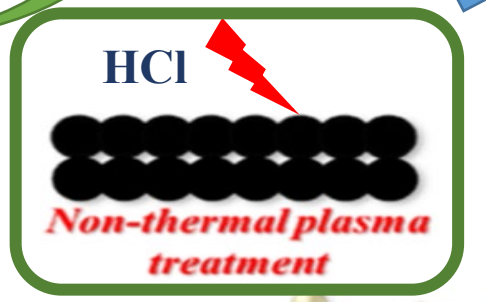

Mercury compounds ❓

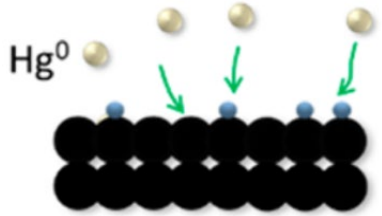

❓ *Mechanism*

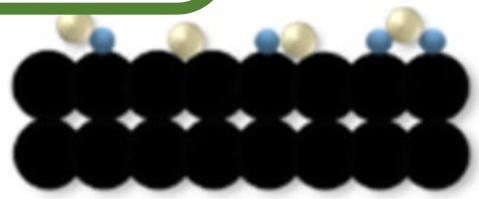

Adsorbed carbonaceous materials

1. Introdution

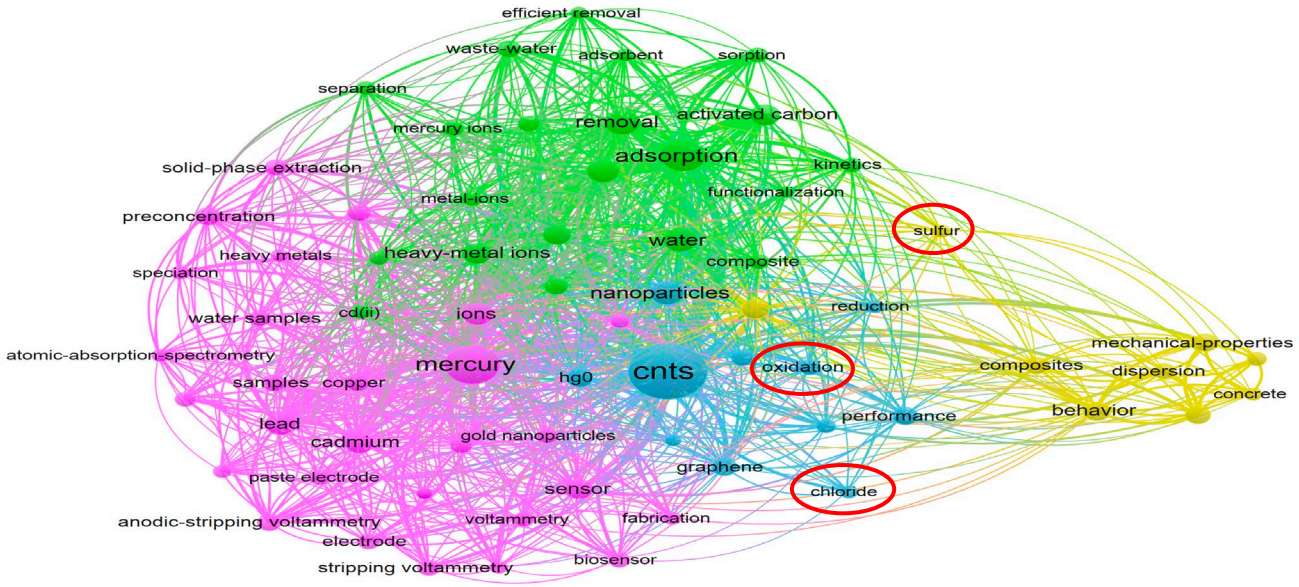

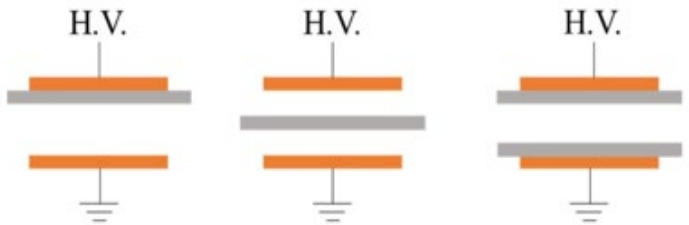

(a) Planar DBD

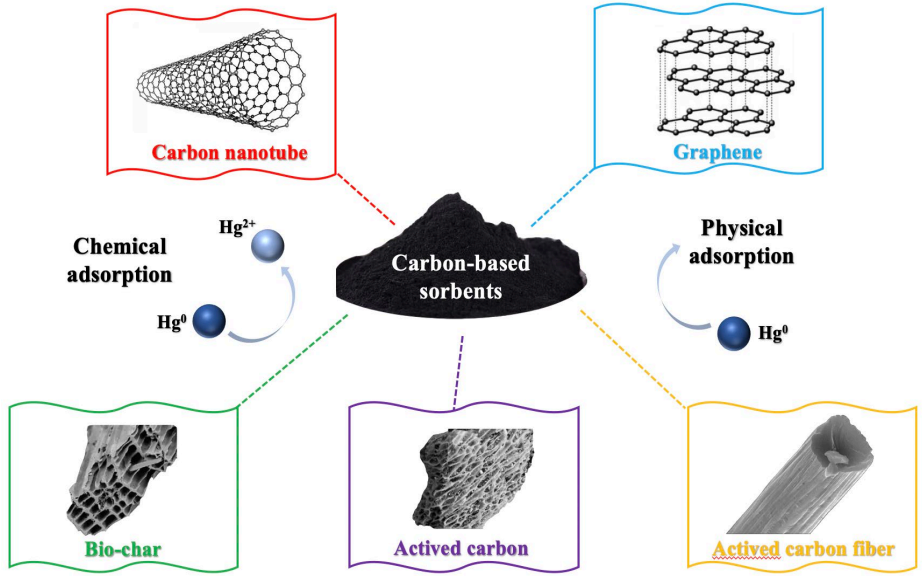

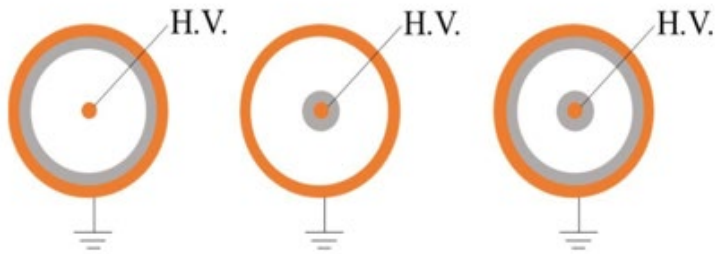

(b) Cylindrical DBD

Electrode Dielectric barrier

2.Methods

装置系统

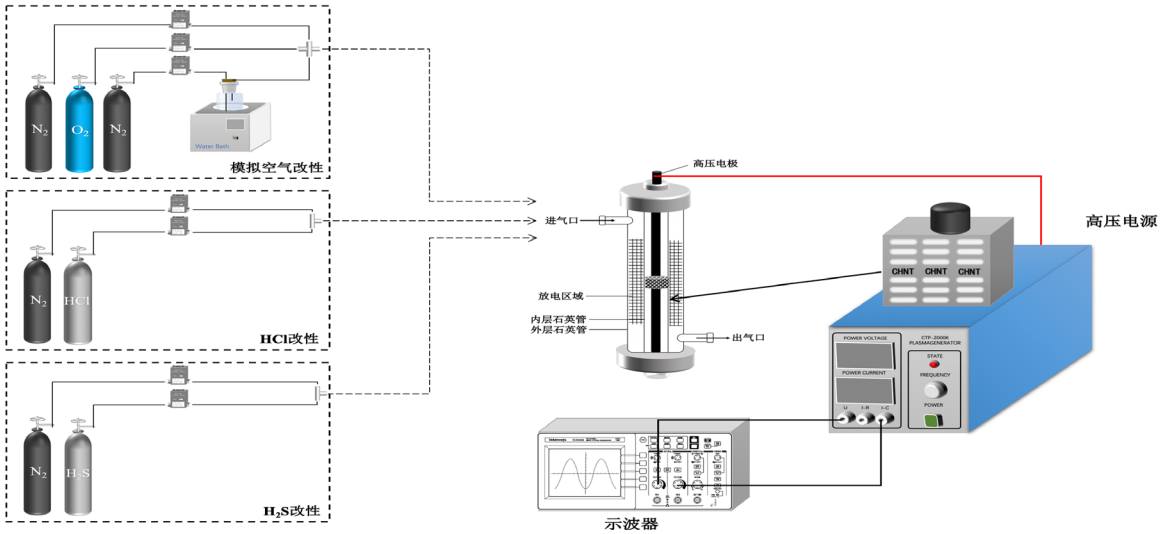

Fig.2-1 Schematic diagram of surface modification

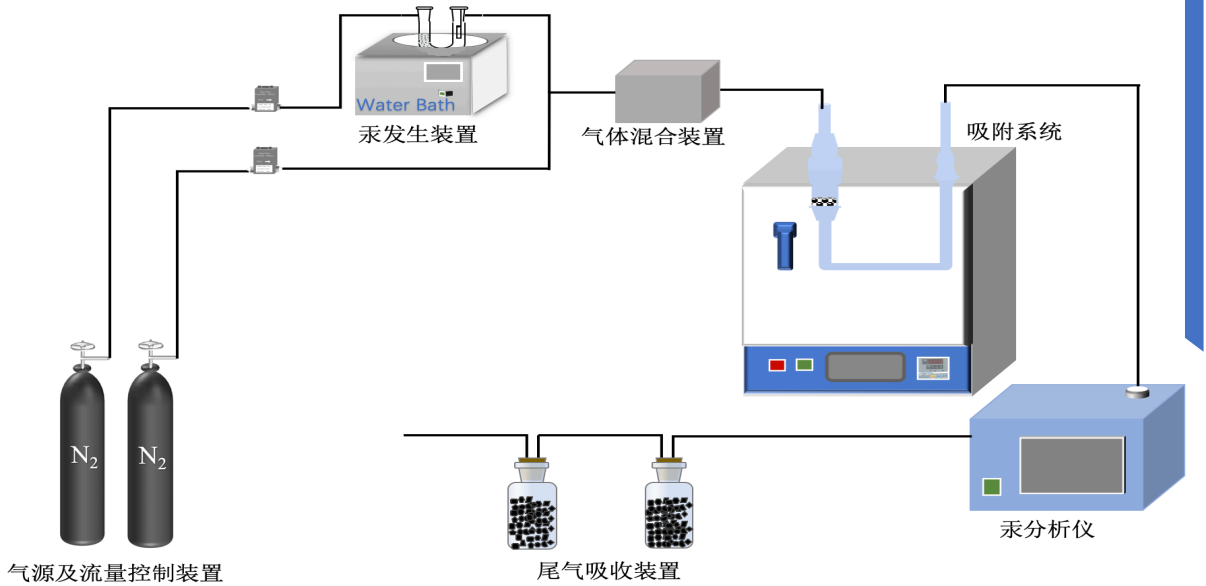

Fig. 2-2 Schematic diagram of adsorption process


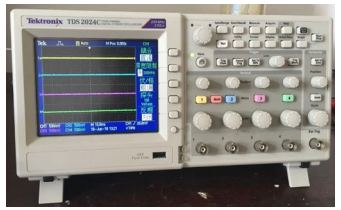


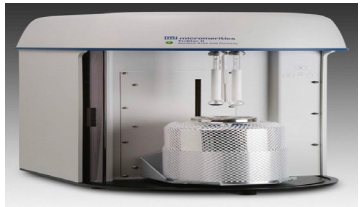

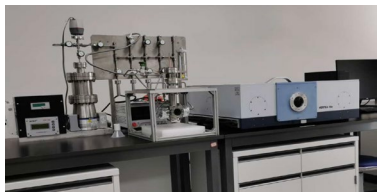


3. Air-plasma Modified CNT

Adsorption

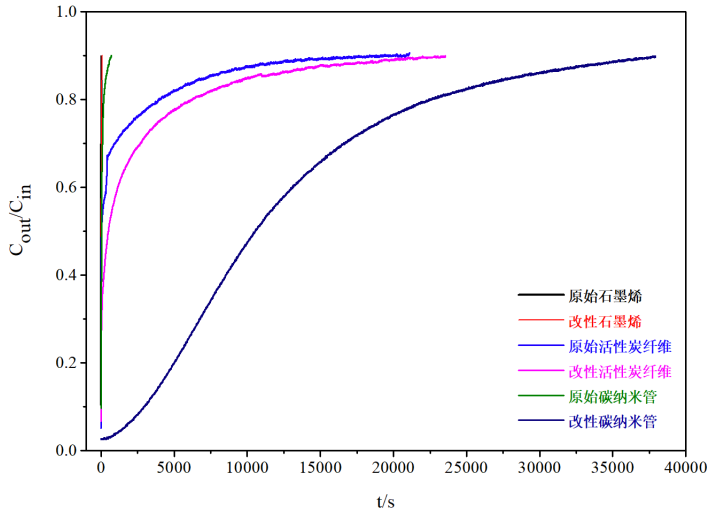

Fig. 3-1 Adsorption Curves of 3 C-materials

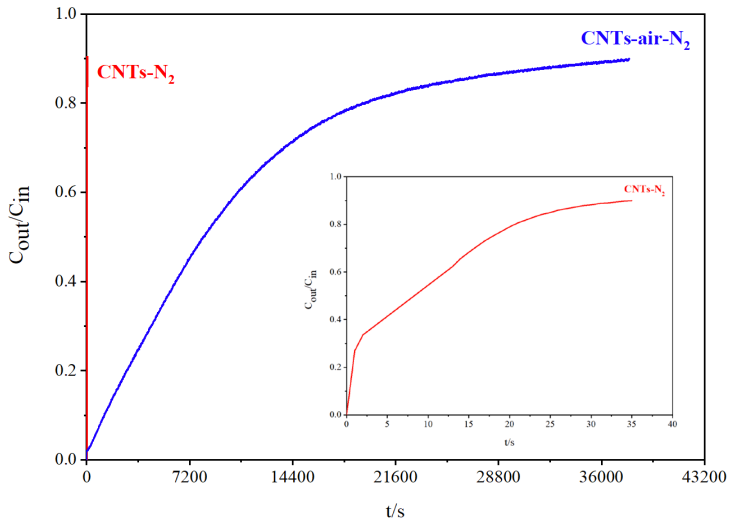

Fig. 3-2 Adsorption Curves of CNTs

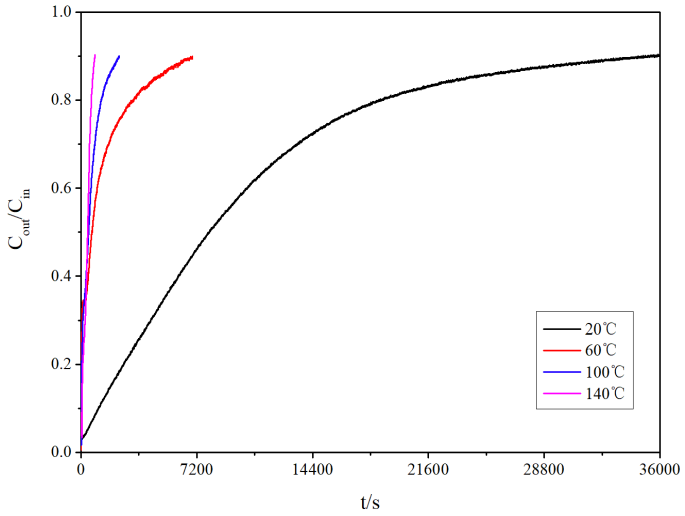

Fig. 3-3 Adsorption Curves of CNTs at different temp

Table 3-1 Adsorption Capacity of CNTs

Sample	Mass (mg)	Breakthrough (%)	Adsorption capacity (μg/g)	Time (s)
carbon nanotube	30.4	90.3	0.52	36
Modified carbon nanotube	30.0	90.0	538.27	37923

3. Air-plasma Modified CNT

厦门大学环境与生态学院
COLLEGE OF THE ENVIRONMENT & ECOLOGY
XIAMEN UNIVERSITY

N_2-Adsorption

Table 3-2 Physical characterization of CNTs

样品	BET Surface Area (m^2/g)	Micropore area (m^2/g)	Micro/total area (%)	Total-pore volume (cm^3/g)	Micropore volume (cm^3/g)	Micro/total volume (%)	Average pore size (Å)
CNTs	313.4907	80.5955	25.7091	1.777674	0.036207	2.0368	23.3841
CNTs-air	265.8807	79.9291	30.0620	1.652354	0.037710	2.2822	26.6305

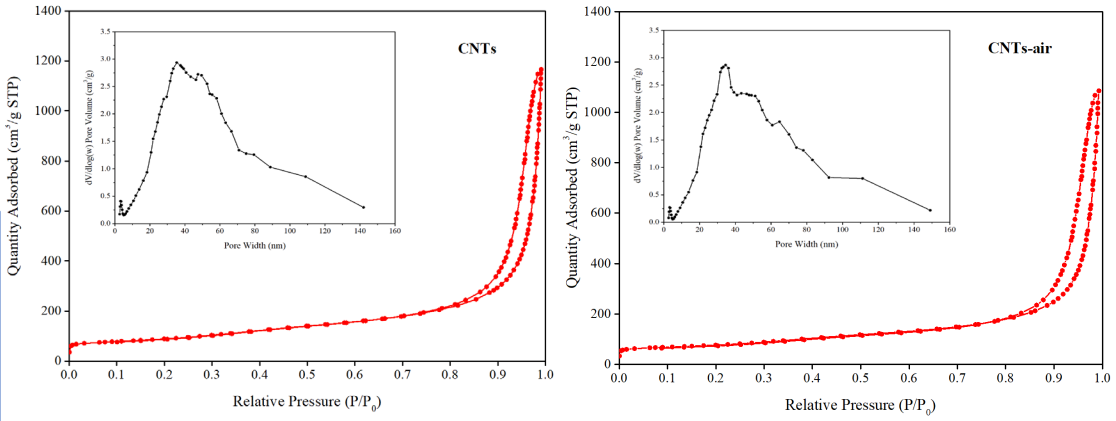

Fig.3-4 N2 adsorption-desorption isotherm of CNTs

- Surface area reduced 15.2%, Average pore size increased 13.9%,
- Pore size distribution is concentrated in 35~40 nm, The pore structure is more uniform
- V-shaped Langmuir isotherm, H4 hysteresis loop, Mesopores
- Micro/total area increased 16.9%, Micro/total volume increased 12%

3. Air-plasma Modified CNT

TEM

CNT	Air-modified CNT	CNT-Hg	Air-modified CNT-Hg
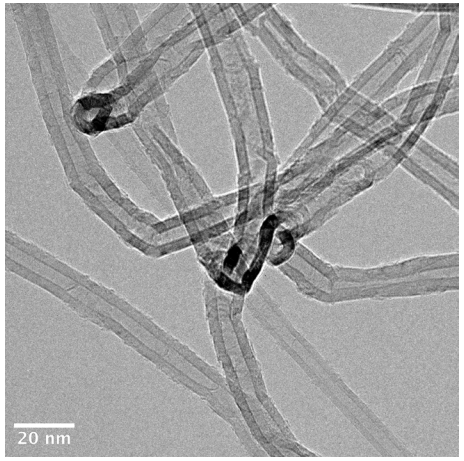	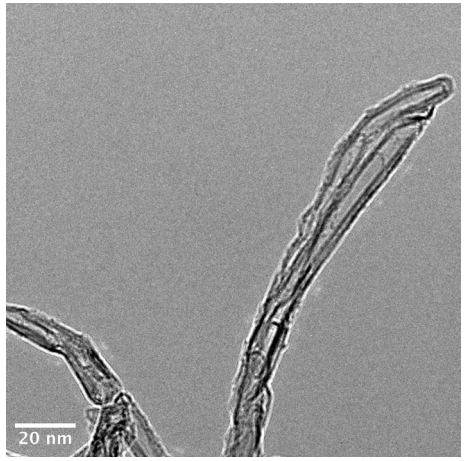	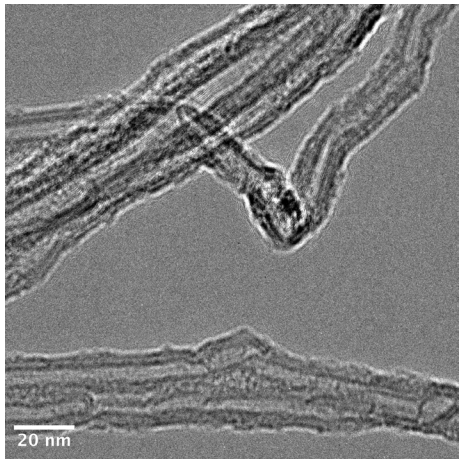	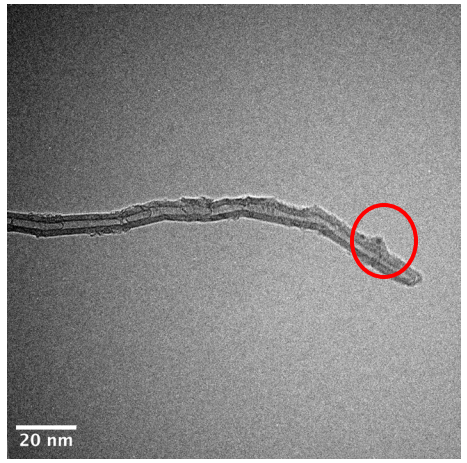

- CNT: smooth surface, no agglomeration, outer diameter:12 nm
- Air-modified CNT: rough surface, shrinkage and cracks on the surface
- Air-modified CNT-Hg: irregular micro-sized particles attached to the tube wall

3. Air-plasma Modified CNT

FT-IR

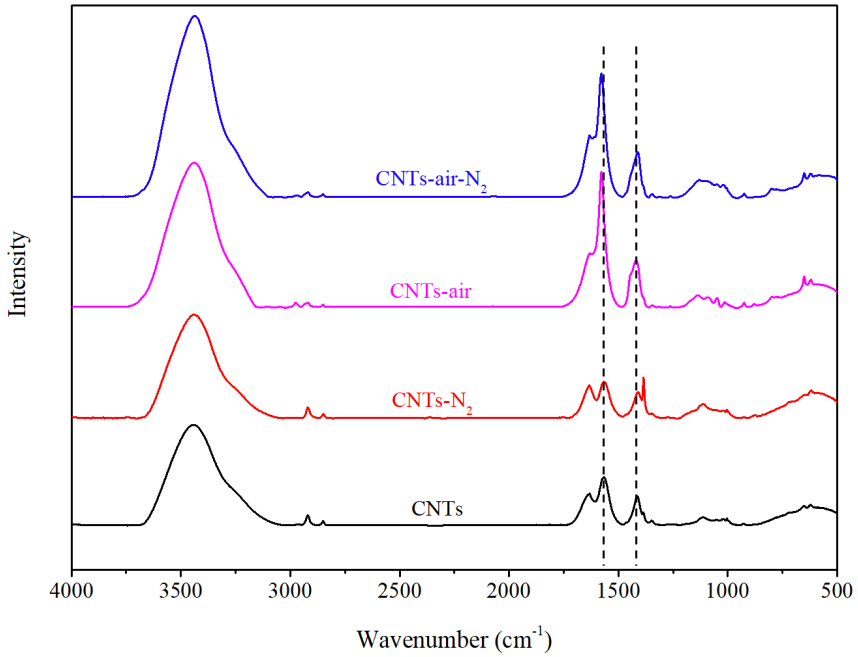

Fig. 3-5 FT-IR spectrums of CNTs

Wavenumber (cm^{-1})	Functional Groups	Wavenumber (cm^{-1})	Functional Groups
3440	-OH	1566	C=O
2918	C-H	1402	-OH
2852	C-H	1384	C-H
1627	-OH	1114	C-O

- CNTs-air: Peak intensity enhanced at 1566 cm^{-1}&1402 cm^{-1}, -OH & C=O increased
- C=O Symmetrical stretching vibration: Ester group, carboxyl group

3. Air-plasma Modified CNT

XPS

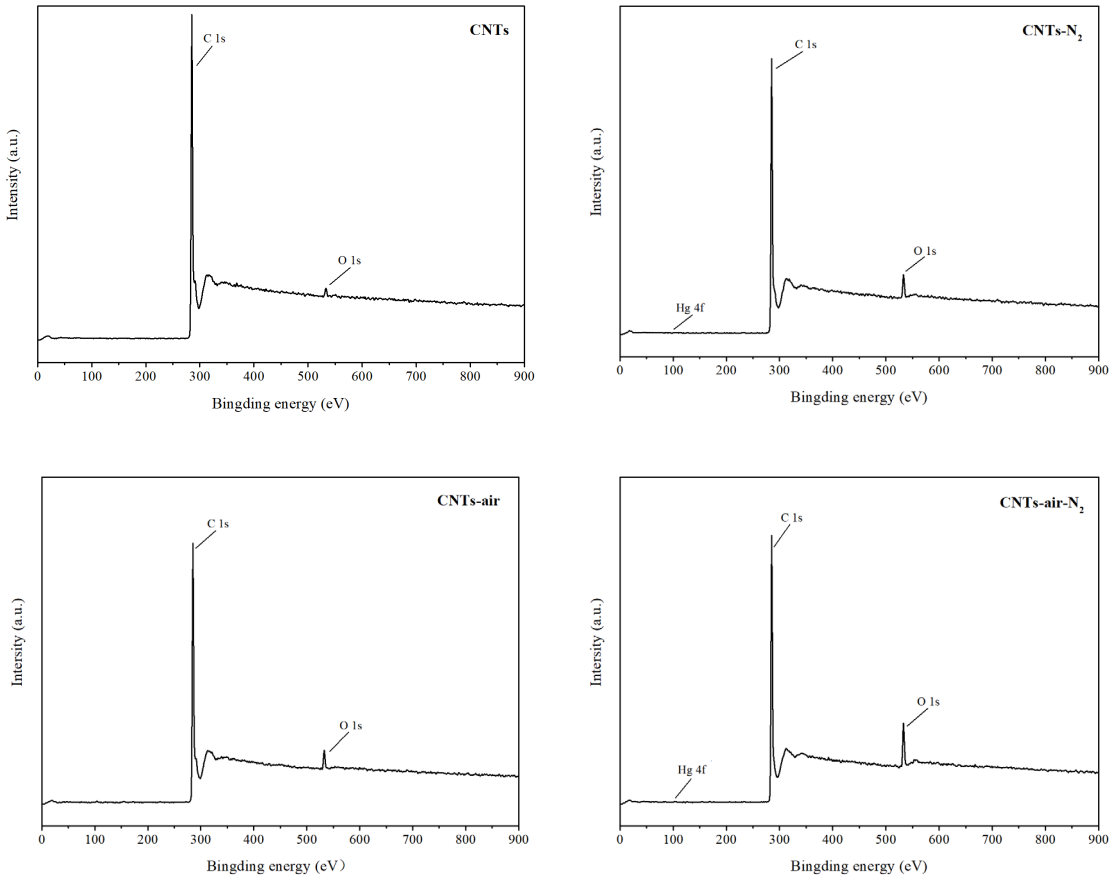

Fig. 3-6 XPS Overall spectrum of CNTs

Table 3-4 Ratio of C 1s、O 1s & Hg 4f of CNTs

碳纳米管	C 1s 284.8	O 1s 532.9	O 1s/C 1s	Hg 103.15
CNTs	98.46	1.54	0.0156	/
CNTs-N_2	96.37	3.63	0.0377	/
CNTs-air	96.72	3.28	0.0339	/
CNTs-air-N_2	92.67	7.12	0.0768	0.21

- O 1s peak rises，with the modifation, effectively increased the oxygen content on the surface of CNTs
- O 1s/C 1s: Surface oxidation degree increased by more than two times

3. Air-plasma Modified CNT

XPS

Table 3-5 Relative peak area integration of C 1s of CNTs

碳纳米管	C 1s			
	284.8 eV	285.6 eV	286.4 eV	288.5 eV
	C-C	C-O	C=O	C-COOH
CNTs	69.40	10.02	10.07	10.51
CNTs-air	64.36	13.90	9.74	12.00
CNTs-N_2	61.94	19.73	14.16	4.16
CNTs-air-N_2	52.41	30.56	11.44	5.58

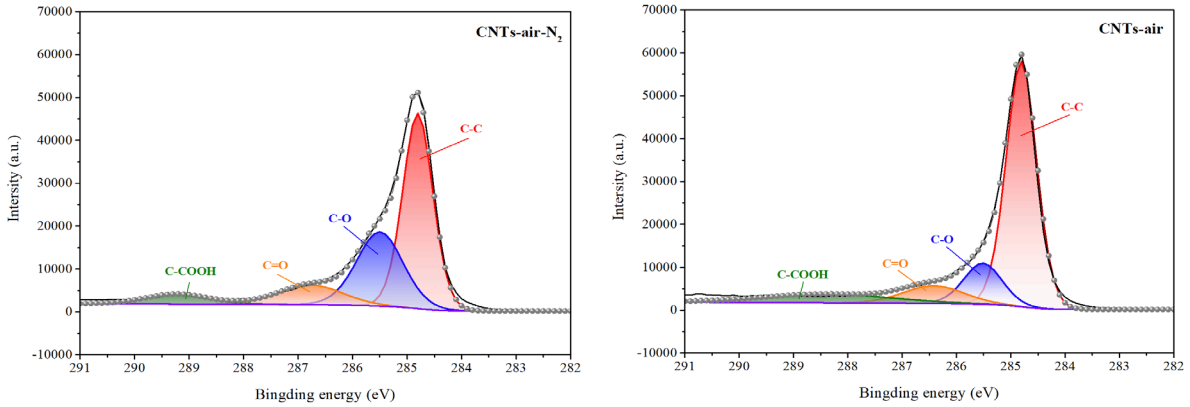

Fig. 3-7 XPS spectrum of C 1s

Table 3-6 Relative peak area integration of O 1s of CNTs

碳纳米管	O 1s			
	531.3	532.3	533.7	534.7
	C=O	C-O	R-O-C=O	C-OOH
CNTs	12.60	34.49	44.15	8.77
CNTs-air	5.96	44.24	39.9	9.91
CNTs-N_2	5.01	47.93	40.11	6.95
CNTs-air-N_2	2.56	47.08	42.50	7.86

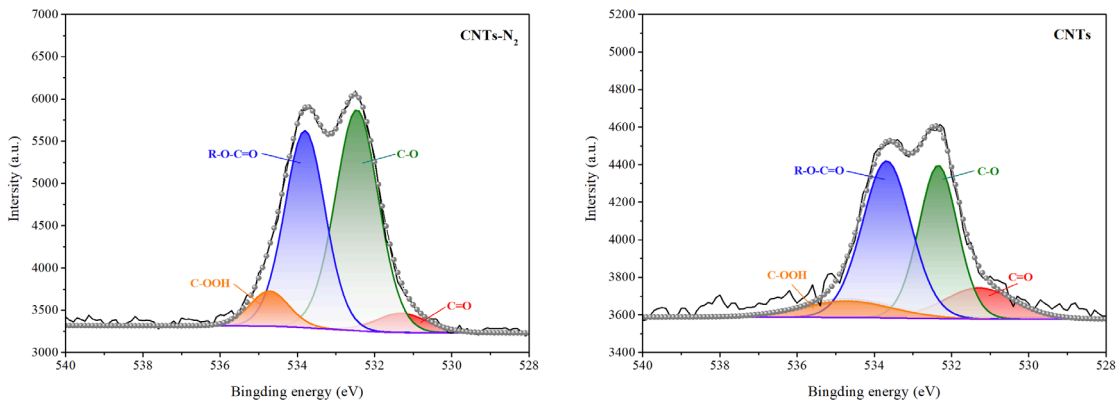

Fig. 3-8 XPS spectrum of O 1s

3. Air-plasma Modified CNT

XPS

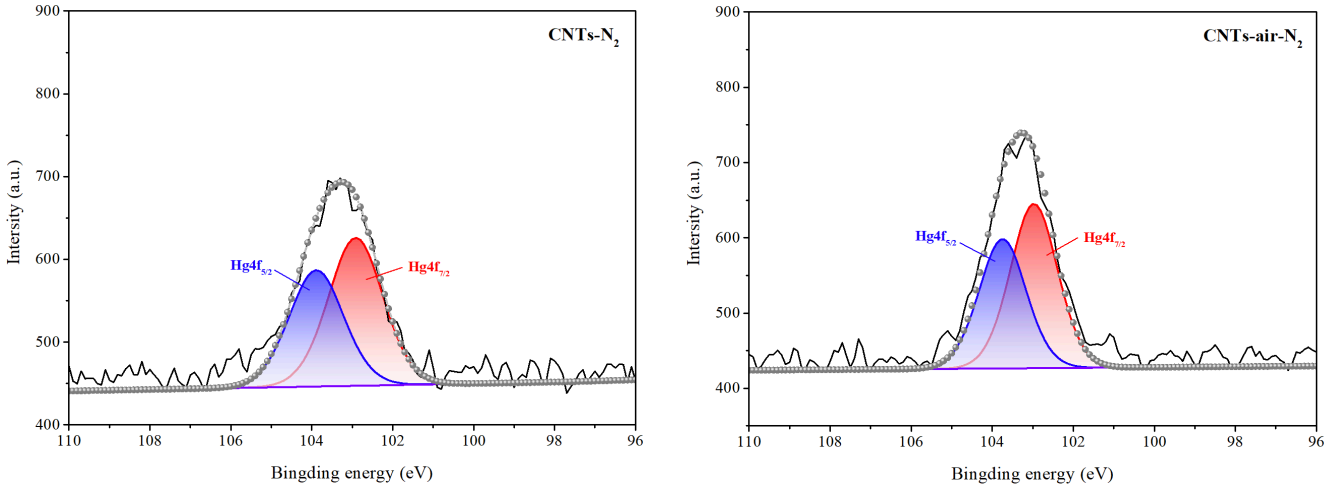

Fig. 3-9 XPS spectrum of Hg 4f

Table 3-7 Relative peak area integration of Hg 4f of CNTs

	Hg 4f	
碳纳米管	97.63	101.95
	Hg 4f 7/2	Hg 4f 5/2
CNTs-N_2	47.66	52.34
CNTs-air-N_2	50.04	49.96

- Hg 4f 7/2 at 97.63 eV and Hg 4f 5/2 at 101.95 eV: Hg^{2+}
- Adsorbed Hg^0 oxidiezed to Hg^{2+} by the Oxygen-containing functional groups at the surface of CNTs

3. Air-plasma Modified CNT

厦门大学环境与生态学院
COLLEGE OF THE ENVIRONMENT & ECOLOGY
XIAMEN UNIVERSITY

XANES

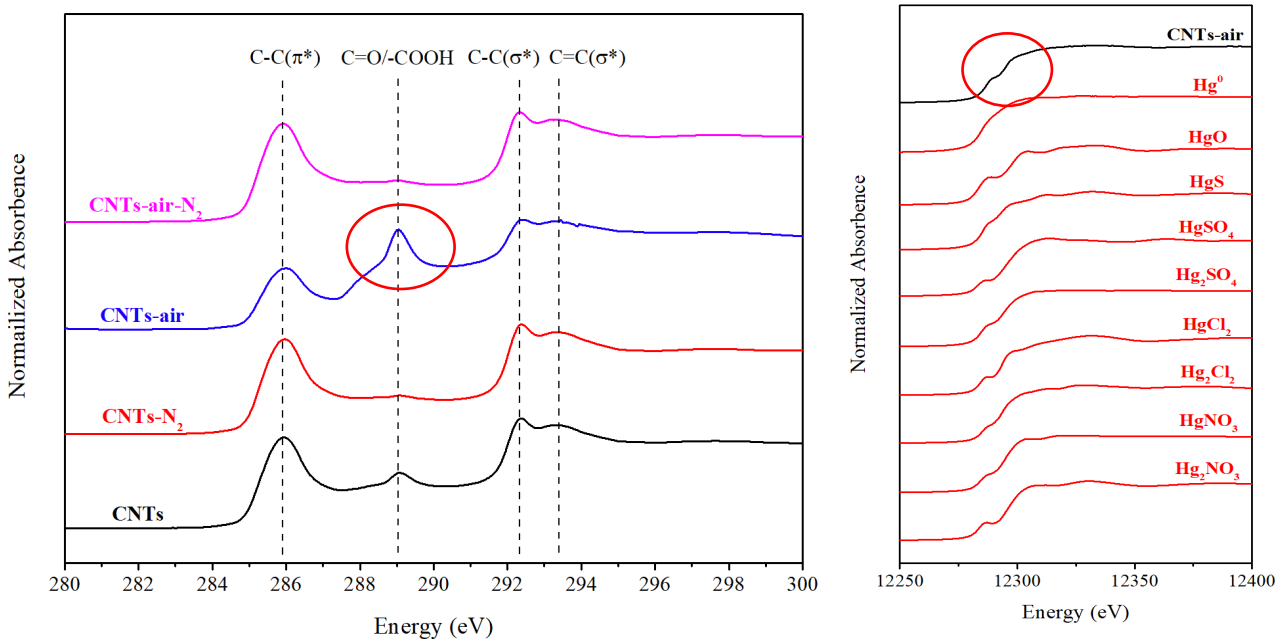

- Absorption peak at 289.1 eV: Ester or carboxyl,
- CNTs-air: peak value increased significantly, C=O. -COOH attached on the surface of CNTs
- CNTs-air-N2 & CNTs-N2: peak value decreased, O-containing groups reacted with Hg^0, and formed HgO
- Two turning points on XANES spectrum: the spectral characteristic of oxidized mercury
- LCF: 79.4％of HgO

Fig. 3-10 XANES spectrum of C & Hg L_{III} of CNTs

Table 3-8 Fraction of chemical species estimated by LCF

Hg-XANES（%）	Hg^0	HgO	HgS	$HgSO_4$	Hg_2SO_4	$HgCl_2$	Hg_2Cl_2	R 因子
CNTs-air-N_2	20.6	79.4	/	/	/	/	/	0.0007559

3. Air-plasma Modified CNT

Characterization

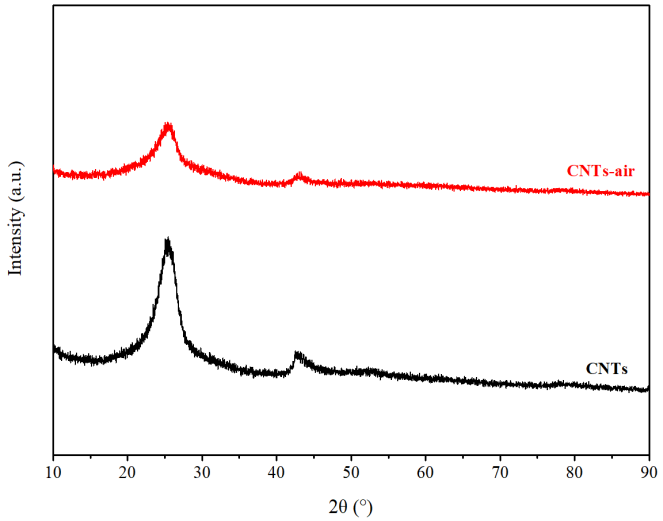

Fig. 3-11 XRD

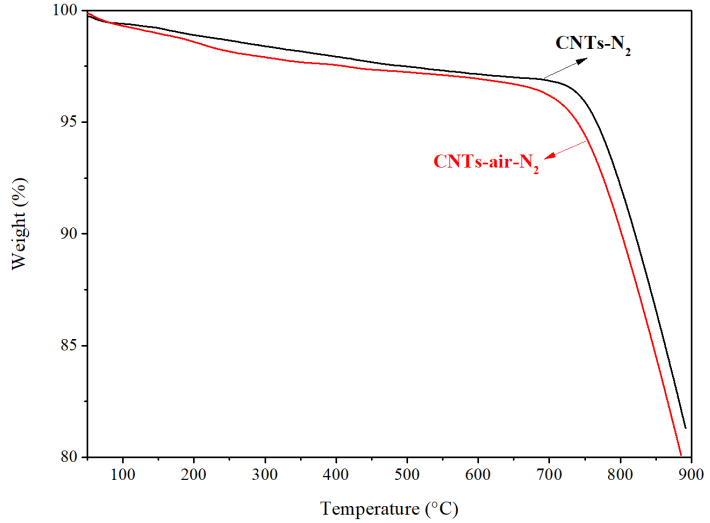

Fig. 3-12 Thermogravimetric Analysis

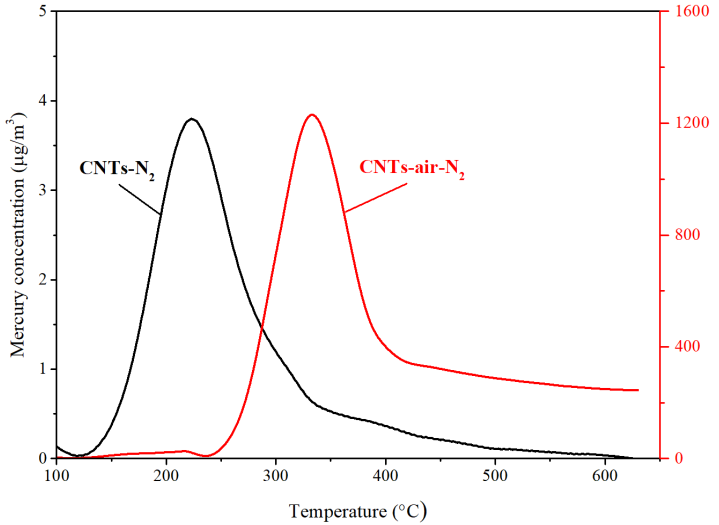

Fig. 3-13 Hg-TPD

- Good graphitization degree: 2θ=26° attributed to Graphite-like structure (002) crystal plane, 2θ=43° corresponds to （100）crystal plane
- Good thermal stability: Heating to 700℃, weight loss of CNTs-N2 3.15%, CNTs-air-N2: 3.81%
- CNTs-N2: Desorption peak at 220℃, Corresponding to the physical adsorption process Hg^0 or HgO
- CNTs-air-N2: Desorption peak at 345℃, from HgO

3. Air-plasma Modified CNT

厦门大学环境与生态学院
COLLEGE OF THE ENVIRONMENT & ECOLOGY
XIAMEN UNIVERSITY

Discharge diagnosis

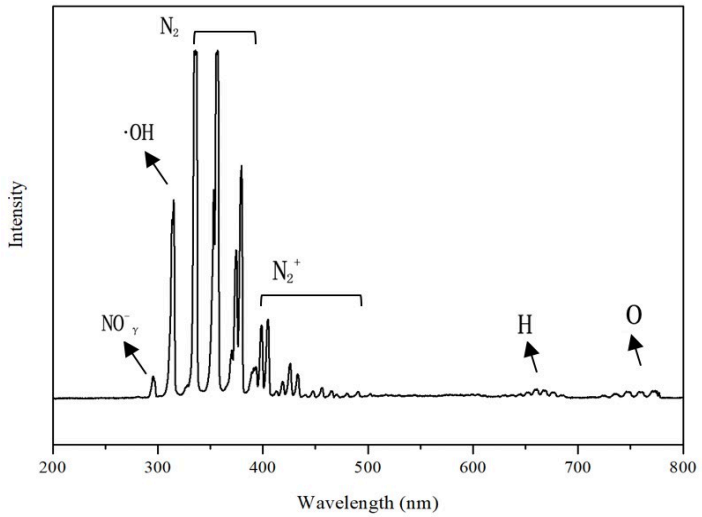

Fig. 3-14Emission spectrum

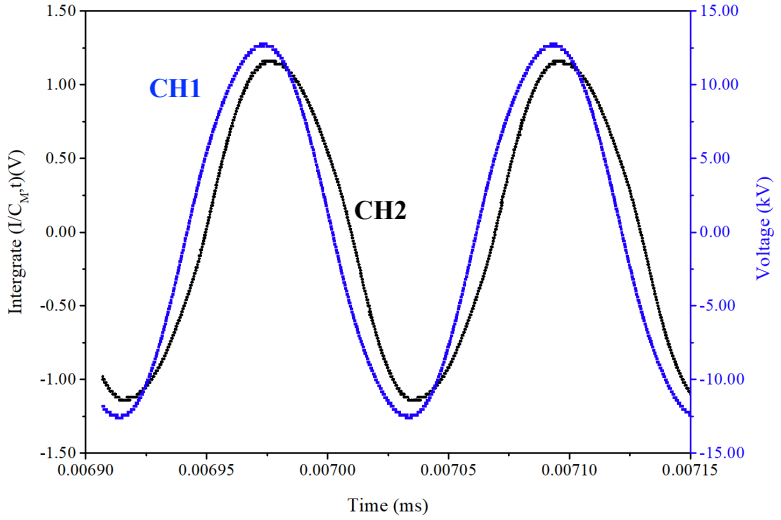

Fig. 3-15 Voltage waveform of DBD&C_M

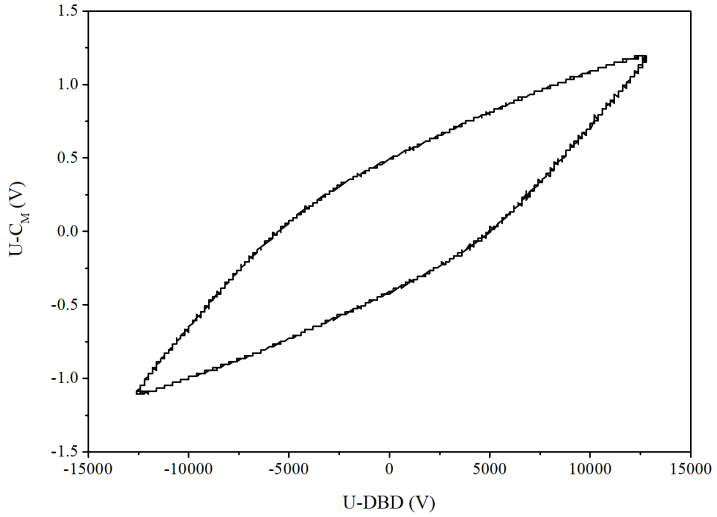

Fig. 3-16 Lissajous curves

Table 3-10 Discharge power of DBD

Voltage（kV）	Actual frequency（Hz）	Area	C_M（μF）	Power（W）
5.0	8298.76	71232	0.47	277.83

Efficient

- Input power: 284.9W
- Energy conversion efficiency :97.52%。

3. Air-plasma Modified CNT

厦门大学环境与生态学院
COLLEGE OF THE ENVIRONMENT & ECOLOGY
XIAMEN UNIVERSITY

Mechanisms

- Modification process of air plasma to CNTs:

$$3O_{2\,(ad)} \xrightarrow{\text{Plasma}} \cdot O + O_3 + O_2^+$$

$$2H_2O_{(ad)} \xrightarrow{\text{Plasma}} \cdot OH + \cdot O + 3\cdot H$$

$$\cdot O + \cdot H \xrightarrow{\text{Plasma}} \cdot OH$$

$$O_2^+ + 2H_2O \xrightarrow{\text{Plasma}} 4\cdot OH$$

$$O_3 + 3H_2O \xrightarrow{\text{Plasma}} 6\cdot OH$$

- Bonding process between O-containing functional groups and CNTs :

$$C + \cdot OH \longrightarrow C\text{-}OH$$

$$-C + \cdot O \longrightarrow -C\text{-}O$$

$$-C + \cdot O \longrightarrow -C{=}O$$

$$-C + \cdot O + \cdot OH \longrightarrow -COOH$$

- Hg^0 adsorption process on CNTs:

$$Hg^0_{(g)} \longrightarrow Hg^0_{(ad)}$$

$$-C\text{-}O + Hg^0_{(ad)} \longrightarrow HgO\text{-}C + \cdot H$$

$$-C{=}O + Hg^0_{(ad)} \longrightarrow HgO\text{-}C + \cdot H$$

$$-OH + Hg^0_{(ad)} \longrightarrow HgO + \cdot H$$

$$-COOH + Hg^0_{(ad)} \longrightarrow -COOHg + \cdot H$$

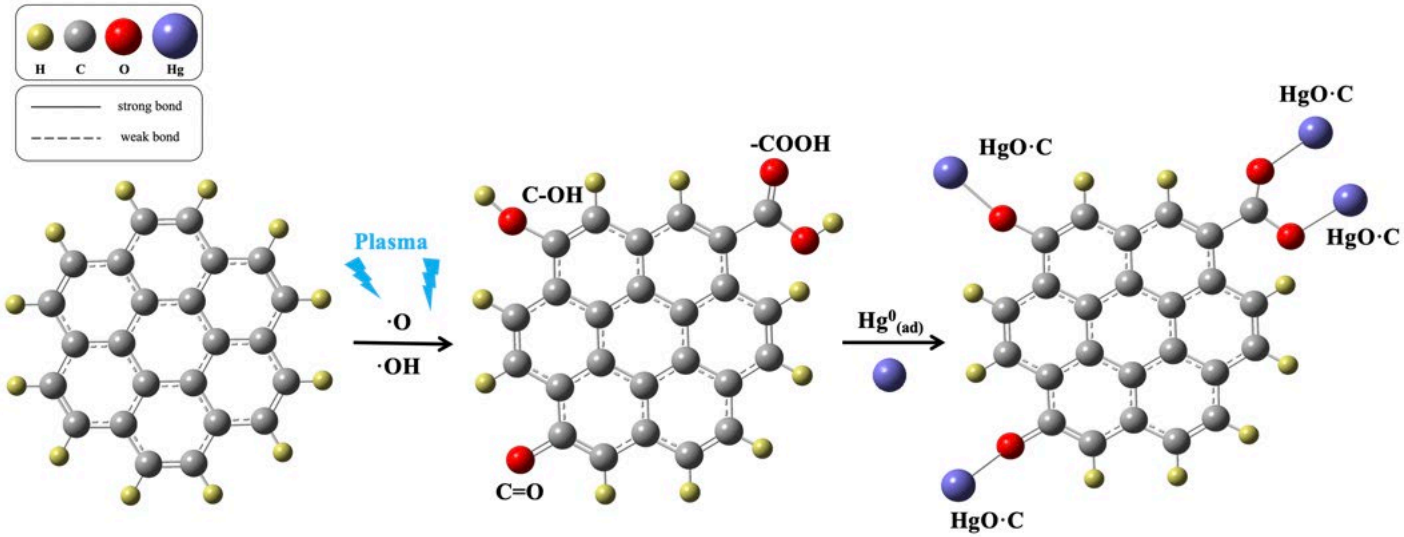

Fig. 3-20 Hg^0 Adsorption mechanisms of CNTs

Conclusion

（1） CNTs modified by DBD plasma

- Surface modification by DBD plasma technology can significantly increased Hg^0 removal efficiency of CNTs, adsorption capacity increased 85、8378、36 times based on temperature。
- Energy conversion efficiency of plasma discharge process is 97.52%
- Air plasma discharge successfully loaded oxygen-containing functional groups on the surface of CNTs

（2）Hg^0 adsorption mechanism of CNTs

- Adsorbed Hg^0 reacted with O-containing functional groups （-OH、-COOH ect.）forms HgO


厦门大学环境与生态学院
COLLEGE OF THE ENVIRONMENT & ECOLOGY
XIAMEN UNIVERSITY
THANK YOU FOR LISTENING
厦门大学环境与生态学院